

# Magnetic water-soluble cyano-bridged metal coordination nano-polymers†

Yannick Guari,<sup>\*a</sup> Joulia Larionova,<sup>\*a</sup> Karine Molvinger,<sup>b</sup> Benjamin Folch<sup>a</sup> and Christian Guérin<sup>a</sup>

Received (in Cambridge, UK) 17th February 2006, Accepted 25th April 2006

First published as an Advance Article on the web 17th May 2006

DOI: 10.1039/b602460b

**Magnetic water-soluble cyano-bridged metallic coordination polymer nanoparticles of controlled size were prepared by using water-soluble chitosan beads.**

Cyano-bridged coordination polymers belong to an important family of molecule-based magnetic materials presenting high critical temperatures and photo-magnetic properties.<sup>1</sup> Indeed, numerous compounds of this family have been synthesised and extensively studied during the last twenty years due to their fundamental interest as well as their bioanalytical and technological applications.<sup>2</sup> In recent years, this research activity was also devoted to the synthesis and studies of these coordination polymer materials at the nano level regime because of their unique physical properties and owing to the need for control over the size, shape and organization for their future incorporation into devices.<sup>3</sup>

A pioneering work on the morphosynthesis of cyano-bridged coordination polymers has been realized by S. Mann and co-workers who obtain cubic nanocrystals with a size ranging from 12 to 50 nm made of Prussian Blue nanoparticles stabilized within micelles.<sup>4</sup> Within the last 5 years, studies devoted to the morphosynthesis of coordination polymers based on cyanometallate building blocks have led to the successful synthesis of nanoparticles of different size by using reverse micelle media,<sup>5</sup> polymers and biopolymers,<sup>6</sup> amorphous and mesostructured silica<sup>7</sup> as matrixes. In this connection, we recently synthesised cyano-bridged metallic nanoparticles by using ionic liquids as structuring media.<sup>8</sup> Nevertheless, no water-soluble biocompatible coordination nanoparticles have been obtained up to date, limiting the use of coordination polymer nanoparticles for bioanalytical applications.

In this communication, we report a new approach to achieve water-soluble magnetic cyano-bridged metallic coordination polymer nanoparticles with a controlled size of 2–3 nm. For this purpose, we apply a two-step approach consisting of growing cyano-bridged metallic coordination polymer nanoparticles inside chitosan beads followed by solubilization of the as-obtained nanocomposite beads in water. Chitosan beads were used in this approach for the following reasons: (i) they contain reactive functional amino groups able to coordinate metal ions that open the way for covalent anchoring of the cyano-bridged metallic

network at the specific sites<sup>9</sup> (Fig. 1S, Supporting Information†), (ii) they have a porous structure<sup>10</sup> that permits a control of the coordination polymer nanoparticle size, (iii) they present high water solubility<sup>9</sup> and (iv) chitosan is biocompatible.

Chitosan beads with porosity as high as 110 m<sup>2</sup> g<sup>-1</sup> were afforded by drying gel beads of the natural polymer chitosan under supercritical CO<sub>2</sub> conditions.<sup>10</sup> Two subsequent treatments of the pristine beads with methanolic solutions of M<sup>2+</sup> and (N(C<sub>4</sub>H<sub>9</sub>)<sub>4</sub>)<sub>3</sub>[Fe(CN)<sub>6</sub>]<sup>11</sup> allowed us to obtain a series of nanocomposite beads M<sup>2+</sup>/[Fe(CN)<sub>6</sub>]<sup>3-</sup>/chitosan (where M<sup>2+</sup> = Ni<sup>2+</sup> for **1a**, Cu<sup>2+</sup> for **2a**, Co<sup>2+</sup> for **3a** and Fe<sup>2+</sup> for **4a**). At each step of the treatment, the chitosan beads were thoroughly washed with methanol and dried *in vacuo*. The atomic ratio M/Fe/chitosan for nanocomposite materials **1a–4a** given by elemental analysis are shown in Table 1. The solubilization of these nanocomposite beads in water (pH = 4–5) gave a series of the respective aqueous solutions **1b–4b**, which were remarkably stable for several months. The dry residues of these solutions contained the same atomic ratio M/Fe as was found in the nanocomposite beads.

The as-obtained nanocomposite beads, as well as the respective aqueous solutions have the colours of the corresponding bulk counterparts: yellow for **1**, red-violet for **2**, violet for **3** and blue for **4** (Fig. 2S, Supporting Information†). Their UV-visible spectra show absorption bands corresponding to inter-metal charge-transfer bands from M<sup>2+</sup> to Fe<sup>3+</sup> of the related bulk compounds (Table 1). No shift of the respective bands is observed after the solubilization of the nanocomposite beads in water (Fig. 3S, Supporting Information†). The IR spectra of the nanocomposites beads **1a–4a** clearly show besides the characteristic bands of chitosan, the bands corresponding to the stretching vibrations of the bridging cyano groups,<sup>12</sup> which can also be found in the spectra of the respective aqueous colloids **1b–4b** (Table 1).

The transmission electronic microscopy (TEM) measurements<sup>13</sup> performed for the nanocomposite beads **1a–4a** clearly show the presence of non-aggregated uniform nanoparticles homogeneously dispersed within the chitosan matrix. The TEM micrograph of **1a** given as an example is shown in Fig. 1a with the histogram of the size distribution, which shows a mean size value of 2.8 nm (insert of Fig. 1a). It should be noted that a narrow nanoparticle size distribution in the range of 2–3 nm is found for all nanocomposites. The TEM observations of the aqueous colloids **1b–4b** also show the presence of uniformly sized spherical shaped nanoparticles, which are non-aggregated and well dispersed in water (Fig. 1b for the sample **1b**). The high resolution transmission electronic microscopy (HRTEM) image performed for the sample **1b** shows the cyano-bridged metallic core of a nanoparticle displaying regular atomic planes demonstrating its crystalline

<sup>a</sup>Laboratoire de Chimie Moléculaire et Organisation du Solide (LCMOS), UMR 5637, Université Montpellier II, Place E. Bataillon, 34095 Montpellier cedex 5, France. E-mail: joulia@univ-montp2.fr; guari@univ-montp2.fr; Fax: (33) 4 67 14 38 52

<sup>b</sup>Laboratoire de Matériaux Catalytiques et Catalyse en Chimie Organique, UMR 5618-CNRS ENSCM, 8 rue de l'École Normale, 34296 Montpellier cedex 5, France

† Electronic supplementary information (ESI) available: Figs. S1–S7. See DOI: 10.1039/b602460b

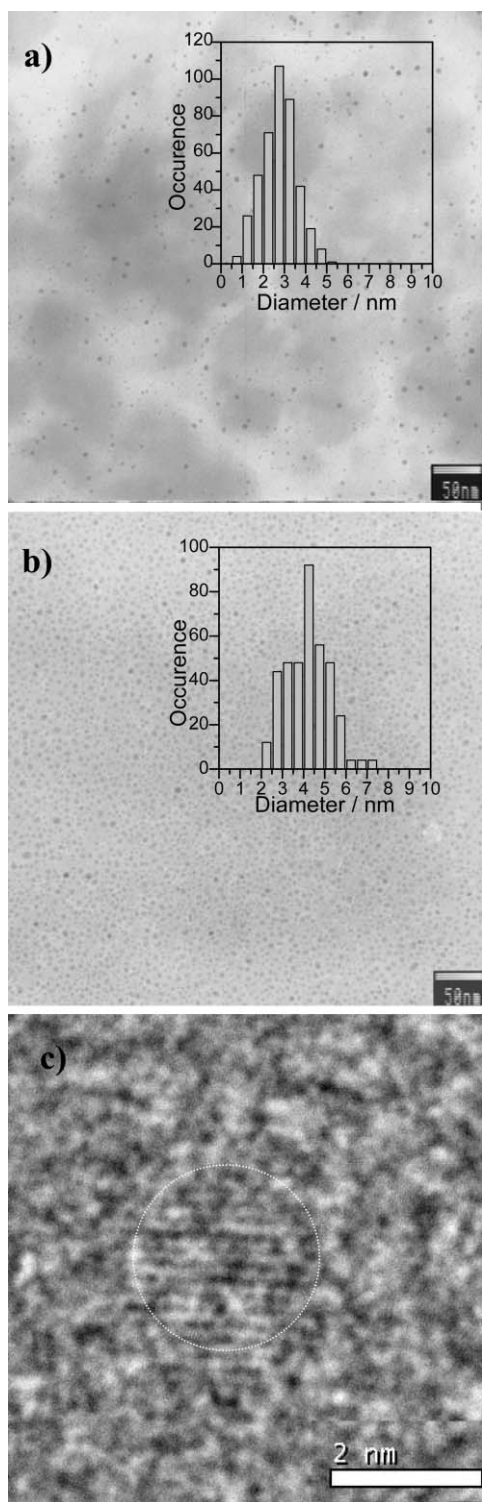


**Fig. 1** (a) TEM image of sample **1a**. The insert shows the size distribution for this sample. (b) TEM image of sample **1b**. The insert shows the size distribution for this sample. (c) HRTEM image of sample **1b** showing the cyano-bridged metallic core of a nanoparticle surrounded with an eye-guide.

nature (Fig. 1c and Fig. 4S, Supporting Information†). As observed, the size distributions of the nanoparticles **1b–4b** are slightly higher than the values observed for the respective nanoparticles in the chitosan matrix. Given these preliminary

results and the fact that the aqueous colloids are astonishingly stable, even when the pH is adjusted to 7, it seems reasonable to presume that after solubilization in water, the cyano-bridged metallic nanoparticles conserve a residual chitosan shell, which prevents their aggregation and precipitation.

The magnetic properties of the aqueous colloids were studied in direct current (dc) and alternating current (ac) modes.<sup>14</sup> Fig. 2 shows the zero field-cooled (ZFC)/field-cooled (FC) magnetization curves in the range of 2–25 K performed for the concentrated colloid **1b** (0.017 M). For the ZFC experiment, the sample was cooled in zero field and then heated in a field of 50 Oe while the net magnetization of the sample was recorded. The FC data were obtained by cooling the sample under a magnetic field of 50 Oe after the ZFC experiments and recording the change in net sample magnetization with temperature. The ZFC curve shows a narrow peak at 11.7 K indicating the blocking temperature of nanoparticles with mean volume. The FC and ZFC curves coincide at high temperatures and start to separate at 13.3 K indicating the blocking temperature of the largest particles. The closeness of the blocking temperature and the temperature of the ZFC/FC curves separation indicates the presence of nanoparticles with a narrow size distribution.<sup>15</sup>

To investigate in more detail the nature of the irreversibility observed in FC/ZFC curves, we studied the temperature dependence of the ac susceptibility, its in-phase ( $\chi'$ ) and the out-of-phase ( $\chi''$ ) components. The temperature dependencies of  $\chi'$  and  $\chi''$  for the concentrated colloid **1b** measured in a zero static field with different frequencies ranging from 1 to 1000 Hz are shown in the insert of Fig. 2. At 1 Hz, responses  $\chi'$  and  $\chi''$  both exhibit a peak, at 12.5 and 11.3 K respectively, which shift toward higher temperature with frequency.<sup>16</sup> The observed frequency dependence may be due to either a pure superparamagnetic regime of the magnetic cyano-bridged nanoparticles or a magnetic regime strongly modified by interparticle interaction, such as a spin glass-like behaviour.<sup>17</sup> Both of these regimes were observed for the colloid systems containing metal or metal oxide nanoparticles.<sup>17–20</sup> The fitting of the thermal variation of the relaxation time with the Arrhenius law,  $\tau = \tau_0 \exp(\Delta/k_B T)$ , where  $\Delta$  is the energy barrier and  $\tau_0$  is the pre-exponential factor does not give reasonable results, suggesting that no pure superparamagnetic regime is observed (Fig. 5S, Supporting Information†).<sup>18</sup> On the contrary, the temperature dependence of the relaxation time can be satisfactory fitted with the spin glass power law,<sup>19</sup>  $\tau = \tau_0 [T_g / (T_{\max} - T_g)]^z$ , with a freezing temperature  $T_g = 11.7$  K, and a critical exponent  $z = 8.9$  and  $\tau_0 = 5.4 \times 10^{-11}$  s (Fig. 6S, Supporting Information†). In addition, the measurements performed on sample **1b** diluted eight times show that the blocking temperature decreases to 9.9 K, indicating that the interparticle interactions strongly influence the magnetic relaxation of the system (Fig. 7S, Supporting Information†).<sup>20</sup>

In this communication we describe the first approach to the synthesis of water-soluble cyano-bridged coordination polymer nanoparticles using chitosan beads as matrix. We show that the porous chitosan beads containing amino functionalities allow control of the growth of the cyano-bridged metallic nanoparticles and provide their covalent anchorage leading to their uniform dispersion. The water solubilization of these nanocomposite beads allows the synthesis of remarkably stable aqueous colloids containing coordination-polymer core–chitosan shell nanoparticles.

**Table 1** Some relevant characteristics for samples 1–4: metal loading, infrared and UV-vis spectroscopy data, size distributions

Sample	Ratio $M^{2+}/[Fe(CN)_6]^{3-}/chitosan^a$	IR, $\nu(CN)/cm^{-1}b$	UV-vis/nm		Nanoparticles size/nm	
			In chitosan	In aqueous solution	In chitosan	In aqueous solution
1	0.59/0.19/1.00 (M = Ni)	2100(s), 2166(w)	436, 726	473, 750	2.8 ± 0.8	4.2 ± 1.0
2	0.47/0.11/1.00 (M = Cu)	2099(s), 2163(w)	425	428	2.2 ± 0.5	5.8 ± 1.1
3	0.47/0.15/1.00 (M = Co)	2099(s), 2165(w)	371, 523, 603(sh)	516, 614(sh)	2.1 ± 0.5	4.0 ± 0.7
4	0.22/1.00 (M = Fe)	2098	467(w), 700	467(w), 700	1.9 ± 0.4	2.7 ± 0.4

<sup>a</sup> Calculated from elemental analysis of 1a–4a. <sup>b</sup> In nanocomposite beads and in aqueous colloids.

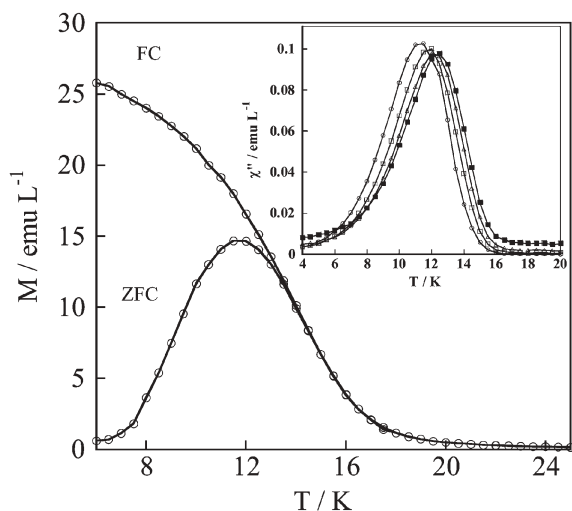


**Fig. 2** Zero field cooled (ZFC)/field cooled (FC) magnetization curves for the sample 1a. Applied field of 50 Oe. Insert: Temperature-dependence of out-of-phase ( $\chi''$ ) component of the ac susceptibility for 1a. Frequencies:

The study of magnetic properties of the colloids shows the appearance of spin glass-like dynamic in these systems. This approach opens a new perspective to the preparation of a large range of biocompatible nanosized water-soluble coordination polymer materials.

The authors thank Mme Corine Reibel (LPMC, Montpellier, France) for magnetic measurements, Mr Lucien Datas (TEMSCAN, Toulouse, France) for HRTEM measurements, Milles Guylhaine Clavel and Hanan Bestal for their help. The authors also thank the CNRS, the Université Montpellier II and the European Network of Excellence Magmanet for financial support.

## Notes and references

- (a) O. Hatlevik, W. E. Buschmann, J. Zhang, J. L. Manson and J. S. Miller, *Adv. Mater.*, 1999, **11**, 914–917; (b) S. M. Holmes and G. S. Girolami, *J. Am. Chem. Soc.*, 1999, **121**, 5593–5599; (c) W. E. Buschmann, S. C. Paulson, C. M. Wynn, M. Girtu, A. J. Epstein, H. S. White and J. S. Miller, *Adv. Mater.*, 1997, **9**, 645–648; (d) T. Mallah, S. Thiébaud, M. Verdaguer and P. Veillet, *Science*, 1993, **262**, 1554–1556; (e) S. Ohkoshi and K. Hashimoto, *J. Am. Chem. Soc.*, 1999, **121**, 10591–10598.
- (a) R. Koncki, *Crit. Rev. Anal. Chem.*, 2002, **32**, 79–96; (b) S. Ayrault, C. Loos-Neskovic, M. Fedoroff and E. Garnier, *Talanta*, 1994, **41**, 1435–1442; (c) L. Roberts, *Science*, 1987, **238**, 1028–1033; (d) D. Wenker, B. Spiess and P. Laugel, *Food Addit. Contam.*, 1990, **7**, 375; (e) H. J. Byker in *Electrochromic Materials II*, vol. 94–2, ed. K. C. Ho and D. A. MacArthur, *The Electrochemical Society*, Pennington, NJ, 1994, pp. 3–12; (f) S. Ferlay, T. Mallah, R. Ouahes, P. Veillet and M. Verdaguer, *Nature*, 1995, **378**, 701.
- E. Dujardin and S. Mann, *Adv. Mater.*, 2004, **16**, 1125–1130.
- (a) S. Vaucher, M. Li and S. Mann, *Angew. Chem., Int. Ed.*, 2000, **39**, 1793–1796; (b) S. Vaucher, J. Fielden, M. Li, E. Dujardin and S. Mann, *Nano Lett.*, 2002, **2**, 225–230.
- L. Catala, T. Gacoin, J.-P. Boilot, E. Riviere, C. Paulsen, E. Lhotel and T. Mallah, *Adv. Mater.*, 2003, **15**, 826–829.
- (a) L. Catala, C. Mathonière, A. Glotter, O. Stephan, T. Gacoin, J.-P. Boilot and T. Mallah, *Chem. Commun.*, 2005, 746–748; (b) L. Catala, A. Glotter, O. Stephan, G. Rogez and T. Mallah, *Chem. Commun.*, 2006, 1018; (c) J. M. Dominguez-Verza and E. Colacio, *Inorg. Chem.*, 2003, **42**, 6983–6985; (d) T. Uemura and S. Kitagawa, *J. Am. Chem. Soc.*, 2003, **125**, 7814–7815.
- (a) G. Clavel, Y. Guari, J. Larionova and Ch. Guérin, *New J. Chem.*, 2005, **29**, 1–7; (b) J. G. Moore, E. J. Lochner, Ch. Ramsey, N. S. Dalal and A. E. Steigman, *Angew. Chem., Int. Ed.*, 2003, **42**, 2741–2743.
- J. Larionova, Y. Guari, G. Clavel and Ch. Guerin, *Chem.–Eur. J.*, 2006, **12**, 3798–3804.
- (a) G. A. F. Roberts, in *Chitin Chemistry*, ed. G. A. F. Roberts, Macmillan Press, Ltd., London, 1992, pp. 54; (b) M. N. V. Ravi Kumar, *React. Funct. Polym.*, 2000, **46**, 1–27; (c) M. N. V. Ravi Kumar, R. A. A. Muzzarelli, C. Muzzarelli, H. Sashiwa and A. J. Domb, *Chem. Rev.*, 2004, **104**, 6017–6084; (d) S. A. Agnihotri, N. N. Mallikarjuna and T. M. Aminabhavi, *J. Controlled Release*, 2004, **100**, 5–28.
- (a) R. Valentin, K. Molvinger, F. Quignard and D. Brunel, *New J. Chem.*, 2003, **27**, 1690–1692; (b) K. Molvinger, F. Auignard, D. Brunel, M. Boissière and J.-M. Devoiselle, *Chem. Mater.*, 2004, **16**, 3367–2272.
- P. K. Mascharah, *Inorg. Chem.*, 1986, **25**, 15–22.
- K. Nakamoto, *Infrared and Raman Spectra*, John Wiley and Sons Inc., New York, 1986.
- Samples for TEM measurements were prepared using ultramicrotomy techniques from resin-embedded powder for the nanocomposite beads 1a–4a and from frozen in liquid nitrogen drops of solutions 1b–4b, and then deposited on copper grids.
- Magnetic susceptibility data were collected with a Quantum Design MPMS-XL SQUID magnetometer working in the 2–350 K temperature range between 0 and 5 T. The magnetic data were corrected for the sample holder and the diamagnetism contributions calculated from the Pascal's constants in *Theory and Applications of Molecular Paramagnetism*, ed. E. A. L. Boudreaux and N. Mulay, John Wiley Sons, New York, 1976.
- D. Bonacchi, A. Caneschi, D. Dorignac, A. Falqui, D. Gatteschi, D. Rovai, C. Sangregorio and R. Sessoli, *Chem. Mater.*, 2004, **16**, 2016–2020.
- The temperature dependencies of the  $\chi'$  and  $\chi''$  components of ac susceptibility of bulk  $Ni_3[Fe(CN)_6]_2$  show no frequency dependent peaks. For instance: ref. 6 and (a) F. Herren, P. Fischer, A. Lüdi and W. Hälg, *Inorg. Chem.*, 1980, **19**, 956–959; (b) V. Cadet, M. Bujoli-Doeuff, L. Force, M. Verdaguer, K. E. Malkhi, A. Deroy, J. P. Besse, C. Chappert, P. Veillet, J. P. Renard and P. Beauvillain, in *Magnetic Molecular Materials*, ed. D. Gatteschi, O. Kahn, J. S. Miller and F. Palacio, NATO ASI Series E, New York, vol. 198, 1991, pp. 281; (c) W. R. Entley, C. R. Treadway and G. S. Girolami, *Mol. Cryst. Liq. Cryst.*, 1995, **273**, 591–604.
- P. E. Jonsson, J. L. Garcia-Palacios, M. F. Hansen and P. Nordblad, *J. Mol. Liq.*, 2004, **114**, 131–135.
- D. Fiorani, J. L. Dormann, J. L. Tholence, L. Bessais and D. Villers, *J. Magn. Magn. Mater.*, 1986, **173–174**, 54–57.
- J. L. Dormann, R. Cherkaoui, L. Spinu, M. Noguès, F. Lucari, F. D'Orazio, D. Fiorani, A. Garcia, E. Tronc and J. P. Jolivet, *J. Magn. Magn. Mater.*, 1988, **177**, L139–L144.
- J. L. Dormann, L. Spinu, E. Tronc, J. P. Jolivet, F. Lucari, F. D'Orazio and D. Fiorani, *J. Magn. Magn. Mater.*, 1998, **183**, L255–L260.